

**Kinetics. Nitrile Insertion.** A  $2.00 \times 10^{-2}$  M solution of **27** was prepared by dissolving 66 mg ( $1.00 \times 10^{-1}$  mmol) of **27** and 15 mg of acenaphthene (internal standard) in  $C_6D_6$  to attain a final volume of 5.00 mL. Each kinetic run was performed by withdrawing a 0.50-mL aliquot of the stock solution, adding a known volume of  $CD_3CN$  via a pipet, and then placing the solution in an NMR tube. The tube was frozen at  $-196^\circ C$  and sealed under vacuum. The tubes were heated in a constant-temperature bath maintained at  $80 \pm 0.2^\circ C$ , and the disappearance of **27** was monitored by  $^1H$  NMR spectroscopy at 300 MHz. Each spectrum was obtained with four scans, allowing an appropriately long (60-s) delay time between each scan. Integration of the 2.30–2.35 ppm multiplet vs the 3.08 ppm singlet of acenaphthene gave the relative concentration of **27**. Standard least-squares analysis of the data obtained afforded  $k_{obs}$  for each run (Table III).

**Reaction of **27** with  $Ph_3P-d_{15}$ .** A  $4.01 \times 10^{-1}$  M stock solution of **27** was prepared by dissolving 53 mg ( $8.02 \times 10^{-2}$  mmol) of **27** and 12.0 mg ( $7.78 \times 10^{-2}$  mmol) of acenaphthene (internal standard) in  $C_6D_6$  to attain a final volume 2.00 mL. A 1.60 M stock solution of  $Ph_3P-d_{15}$  was prepared by dissolving 444 mg (1.60 mmol) of  $Ph_3P-d_{15}$  in  $C_6D_6$  to attain a final volume of 1.00 mL. This solution was used to prepare solutions of  $8.00 \times 10^{-1}$  and  $4.00 \times 10^{-1}$  M by successive dilution of 0.50-mL aliquots of the 1.60 and  $8.00 \times 10^{-1}$  M solutions to 1.00 mL. Each kinetic run was performed by transferring a 0.25-mL aliquot of the solution of **27** to septum-capped NMR tube and adding a 0.25-mL aliquot

of  $8.00 \times 10^{-1}$  or  $4.00 \times 10^{-1}$  M  $Ph_3P-d_{15}$  solution by syringe. The solutions were mixed quickly, and the tube was immediately placed in the NMR probe maintained at  $25 \pm 0.5^\circ C$ . The initial spectrum was obtained after allowing temperature stabilization of the solution. All spectra were obtained at 300 MHz with one scan at appropriate time intervals and were analyzed identically with those above. Rate constants are given in Table IV.

**Acknowledgment.** We are grateful for financial support of this work from the National Institutes of Health (Grant No. GM 35699).

**Registry No.** 1, 96413-81-9; 2, 104067-89-2; 3, 124342-53-6; 4, 124342-54-7; 5, 14220-21-4; 6, 15259-18-4; 7, 124378-87-6; **8a**, 96413-82-0; **8b**, 124378-88-7; **9a**, 124342-55-8; **9b**, 124378-89-8; **10a**, 124342-56-9; **10b**, 124378-90-1; **11a**, 124342-57-0; **11b**, 124378-91-2; **12a**, 124342-58-1; **12b**, 124378-92-3; **13a**, 124342-59-2; **13b**, 124378-93-4; **14a**, 124342-60-5; **14b**, 124378-94-5; **15**, 124342-61-6; **17**, 124342-62-7; **18**, 124342-63-8; **19**, 96427-38-2; **20**, 124342-64-9; **21**, 124342-65-0; **22**, 124342-66-1; **23**, 124354-99-0; **24**, 124342-67-2; **25**, 124342-68-3; **26**, 124342-69-4; **27**, 124342-70-7; **28**, 124342-71-8; **35**, 124342-72-9; **36**, 124342-73-0; **41**, 124342-74-1;  $TfOCH_2CO_2Et$ , 77902-90-0;  $Re_2(CO)_{10}$ , 14285-68-8;  $MsOCH(CH_3)CO_2Et$ , 58742-64-6;  $CH_3CH_2CN$ , 107-12-0;  $CH_3CN$ , 75-05-8;  $(CH_3)_2CHCN$ , 78-82-0;  $C_6H_5CN$ , 100-47-0; trifluoromethanesulfonic anhydride, 358-23-6; ethyl lactate, 97-64-3; ethyl chloroacetate, 105-39-5; chloroacetone, 78-95-5; 2-chloroacetophenone, 532-27-4; *tert*-butyl chloroacetate, 107-59-5; 2-chloro-*N,N*-diethylacetamide, 2315-36-8; chloroacetonitrile, 107-14-2.

(50) Bianco, V. D.; Doronzo, S. *Inorg. Synth.* 1976, 16, 164-6.

## Insertion, H/D Exchange, and $\sigma$ -Bond Metathesis Reactions of Acetylene with $Cl_2ScH$

A. K. Rappé

Department of Chemistry, Colorado State University, Fort Collins, Colorado 80523

Received November 25, 1988

Correlated ab initio theoretical calculations at the valence double- $\zeta$  plus polarization level are used to study reaction paths for the reaction of acetylene with  $Cl_2ScH$ . The paths studied are the classic insertion pathway and two  $\sigma$ -bond metathesis pathways, one resulting in H/D exchange and the other resulting in formation of a scandium acetylide. The insertion process is calculated to have a barrier of 6.3 kcal/mol with respect to the complexed acetylene ( $-9.1$  kcal/mol with respect to free acetylene) and to be 36.5 kcal/mol exothermic with respect to free acetylene. The direct H/D exchange reaction is calculated to have a barrier of 13.7 kcal/mol with respect to free acetylene. The acetylide-forming reaction is calculated to have a barrier of 6.2 kcal/mol with respect to free acetylene and to be 15.2 kcal/mol exothermic with respect to free acetylene. Given the reversibility of this reaction, H/D exchange could occur through sequential formation and reduction of the acetylide complex. The insertion pathway is the only one calculated to proceed through a metal acetylene complex. The two  $\sigma$ -bond metathesis pathways are each calculated to proceed through a direct interaction with the Sc-H bond. In addition, the overall reaction energetics are calculated for the insertion and acetylide formation reactions of  $Cl_2ScCH_3$  with acetylene. In contrast to the hydride reactions, the insertion and acetylide formation reactions for the methyl complex are found to be equivalently exothermic. The insertion reaction is calculated to be 39.1 kcal/mol exothermic and the acetylide formation reaction is calculated to be 40.9 kcal/mol exothermic.

### Introduction

The activation of carbon-carbon and carbon-hydrogen bonds of saturated and unsaturated hydrocarbons by transition metals is a major goal of experimental organometallic chemistry.<sup>1-6</sup> This activation would provide synthetic organic chemists with a new array of reagents

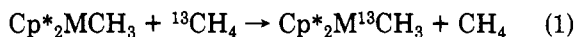
for selective syntheses as well as providing new schemes for the upgrading of fuel stocks. There have been recent successes in the activation of carbon-hydrogen bonds.<sup>1,2</sup> For example, degenerate methane exchange or  $\sigma$ -bond

(1) (a) Thompson, M. E.; Bercaw, J. E. *Pure Appl. Chem.* 1984, 56, 1-11. (b) Bercaw, J. E.; Davies, D. L.; Wolczanski, P. T. *Organometallics* 1986, 5, 443-450. (c) Thompson, M. E.; Baxter, S. M.; Bulls, A. R.; Burger, B. J.; Nolan, M. C.; Santarsiero, B. D.; Schaefer, W. P.; Bercaw, J. E. *J. Am. Chem. Soc.* 1987, 109, 203-219. (d) Bunel, E.; Burger, B. J.; Bercaw, J. E. *J. Am. Chem. Soc.* 1988, 110, 976-978.

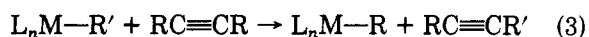
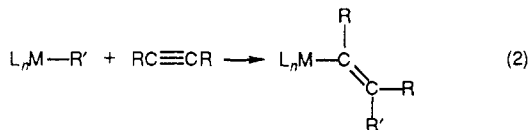
(2) Watson, P. L. *J. Am. Chem. Soc.* 1982, 104, 337-339. Watson, P. L. *J. Chem. Soc., Chem. Commun.* 1983, 276-277. Watson, P. L. *J. Am. Chem. Soc.* 1983, 105, 6491-6493. Watson, P. L.; Parshall, G. W. *Acc. Chem. Res.* 1985, 18, 51-56.

(3) (a) Stoutland, P. O.; Bergman, R. G. *J. Am. Chem. Soc.* 1985, 107, 4581. (b) Silvestre, J.; Calhorda, M. J.; Hoffmann, R.; Stoutland, P. O.; Bergman, R. G. *Organometallics* 1986, 5, 1841-1851. (c) Stoutland, P. O.; Bergman, R. G. *J. Am. Chem. Soc.* 1988, 5732-5744, and references therein.

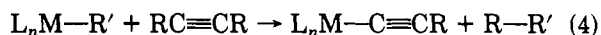
metathesis has been observed for group 3 transition metal complexes<sup>1</sup> as well as lanthanide<sup>2</sup> complexes:



where  $M = Sc, Y,$  and  $Lu,$  and  $Cp^* = \eta^5-C_5Me_5$  (penta-methylcyclopentadienyl). The activation of alkenyl, aryl, and alkynyl C-H bonds<sup>1</sup> has also been observed. A covalent four-center 2 + 2 transition state has been proposed to explain the greater reactivity of sp over sp<sup>2</sup> over sp<sup>3</sup> bonds.<sup>1</sup> The reactions of alkenes and alkynes with metal-hydrogen and metal-carbon bonds are of special interest because alternate pathways are observed.<sup>1</sup> The metal-hydrogen or metal-carbon  $\sigma$  bond can either insert into one of the  $\pi$  bonds through the classical  $\beta$  insertion pathway: participate in  $\sigma$ -bond metathesis:



or simply undergo a  $\sigma$ -bond metathesis exchange resulting in C-C bond coupling:



It is of interest to probe the electronic and geometric factors that favor one pathway over another.

Finally, recent experiments<sup>1,3</sup> have raised questions regarding the effect of prior coordination of a  $\pi$  bond on activation processes.<sup>1,3</sup> In an elegant series of experiments, Stoutland and Bergman<sup>3</sup> have shown that ethylene reacts with the coordinatively unsaturated intermediate  $Cp^*Ir(PMe_3)$  to preferentially form a vinyl hydride rather than the expected olefin adduct (kinetic ratio at 130 °C is 66/34). The vinyl hydride can subsequently be converted quantitatively to the olefin adduct at 200 °C, indicating that the olefin adduct is indeed the thermodynamic product. Further, since the olefin adduct is observed to be stable under the insertion reaction conditions, it cannot be on the reaction path for formation of the vinyl hydride. This preferential formation of a product that occurs through a reaction path that must have an intrinsic activation barrier (breakage and formation of covalent bonds), instead of a product that occurs through a reaction path that is recognized to involve very little electronic reorganization, runs counter to both intuition and theoretical studies.<sup>3b</sup> Extended Hückel calculations suggest that the vinyl hydride forming reaction has a barrier at least 10 kcal/mol larger than that for forming the olefin adduct.

Bercaw and co-workers<sup>1</sup> have observed that  $Cp^*_2Sc-R'$  ( $R' = H, CH_3$ ) reacts with propyne to form exclusively the  $\sigma$ -bond metathesis product acetylide instead of the classical  $\beta$ -insertion product. If prior coordination of the  $\pi$  bond

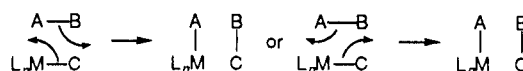
does activate the  $\pi$  bond, then the activation energy for the insertion reaction should be lower than for the  $\sigma$ -bond metathesis reaction—all other factors being equal (they certainly are not, but  $\beta$  insertion is far more common than  $\sigma$ -bond metathesis).

In the present study we compare the classical  $\beta$ -alkyne insertion pathway (2) with the  $\sigma$ -bond metathesis pathway (3) and with the acetylide forming reaction (4). For our work we use  $M = Sc, R = H,$  and  $R' = H, CH_3$ . The classical  $\beta$ -alkyne insertion pathway (2) is experimentally observed with internal alkynes ( $R = CH_3$ ) but not with terminal alkynes ( $R = H$ ). The  $\sigma$ -bond metathesis pathway (3) is not observed for alkynes. The acetylide forming reaction (4) is not experimentally observed with internal alkynes ( $R = CH_3$ ) but is observed with terminal alkynes ( $R = H$ ). For each reaction we have determined the equilibrium geometries and relative reaction energetics. In addition, for  $R$  and  $R'$  equal to  $H,$  we have determined the saddlepoint geometries and activation energetics. We have chosen to model the experimental  $Cp^*_2Sc$  systems with  $Cl_2Sc$  in order to compare the results of this study with previous theoretical work on related complexes.<sup>4</sup> Although the energetic and geometric results obtained with the model system should not be in quantitative agreement with the experimental results, they should provide an appropriate conceptual basis for discussing the experimental results.

## Results

In section I we will discuss the general electronic reorganization that we have found to be common to all four-center 2 + 2 reactions containing a transition metal d orbital.<sup>4</sup> A comparison of the electronic and geometric reorganizations observed for reactions 2-4 is presented in section II. The calculated reaction energetics are presented in section III. The discussion and overall conclusions are given in section IV, and the theoretical details are supplied in section V.

**I. General Four-Center 2 + 2 Electronic Reorganization.** The orbital reorganization common to the theoretical studies of metal-containing four-center 2 + 2 reactions published to date<sup>4</sup> is



The bond between centers A and B in the reactant is converted into a bond between centers B and C in the product. In response to this, the bond between M and C in the reactant is transformed into a bond between centers M and A in the product. If there is a significant energy difference between the AB bond and the MC bond, then the stronger bond (usually AB) is transformed with minimal orthogonality constraints. The weaker bond (usually between M and C) builds in Pauli principle induced orthogonality constraints to the AB (reactant) or BC (product) bonding orbital. Independent of the direction of electron flow there are always two centers (usually M and B) whose one-electron orbitals remain on their original centers and two centers whose one-electron orbitals move during the course of reaction. If "symmetry" (e.g., ethylene plus ethylene or ethylene plus formaldehyde) precludes this localization, the reactions have a high activation energy.<sup>4e,f</sup>

Usually, the one-electron orbital on center B remains on center B during the course of the reaction. The one-electron orbital on center A moves to center C without additional nodes and near the transition state is symme-

(4) (a) Steigerwald, M. L.; Goddard, W. A. *J. Am. Chem. Soc.* 1984, 106, 308-311. (b) Upton, T. H. *J. Am. Chem. Soc.* 1984, 106, 1561-1571. (c) Fujimoto, H.; Yamasaki, T.; Mizutani, H.; Koga, N. *J. Am. Chem. Soc.* 1984, 106, 6157-6161. (d) Koga, N.; Obara, S.; Kitauro, K.; Morokuma, K. *J. Am. Chem. Soc.* 1984, 106, 7109-7116. (e) Rappé, A. K.; Upton, T. H. *Organometallics* 1984, 3, 1440-1442. (f) Upton, T. H.; Rappé, A. K. *J. Am. Chem. Soc.* 1985, 107, 1206-1218. (g) Koga, N.; Obara, S.; Kitauro, K.; Morokuma, K. *J. Am. Chem. Soc.* 1985, 107, 7109-7116. (h) Rabaã, H.; Sailard, J.-Y.; Hoffmann, R. *J. Am. Chem. Soc.* 1986, 108, 4327-4333. (i) Rappé, A. K. *Organometallics* 1987, 6, 354-357. (j) Williamson, R. L.; Hall, M. B. *J. Am. Chem. Soc.* 1988, 110, 4428-4429.

(5) Thorn, D. L.; Hoffmann, R. *J. Am. Chem. Soc.* 1978, 100, 2079-2090.

(6) Albright, T. A.; Burdett, J. K.; Whangbo, M.-H. *Orbital Interactions in Chemistry*; Wiley: New York, 1985. Collman, J. P.; Hegedus, L. S.; Norton, J. R.; Finke, R. G. *Principles and Applications of Organotransition Metal Chemistry*; University Science Books: Mill Valley, CA, 1987.

Table I. Molecular Coordinates and CI Total Energies<sup>a</sup>

atom	X	Y	Z	atom	X	Y	Z
(a) Cl <sub>2</sub> ScH							
CI Total Energy = -965.658 779							
Sc	0.0	0.0	0.570 279 886	Cl2	2.140 057 45	0.0	-0.394 630 966
Cl1	-2.140 057 45	0.0	-0.394 630 966	H	0.0	0.0	2.325 665 18
(b) Cl <sub>2</sub> ScH·C <sub>2</sub> H <sub>2</sub> Reactant							
CI Total Energy = -1 042.653 625							
Sc	0.0	0.514 305 482	-0.073 902 5525	C2	0.0	0.264 092 601	2.745 320 1
Cl1	-2.078 470 92	-0.248 339 719	-0.890 127 107	H1	0.0	2.199 910 94	0.460 281 937
Cl2	2.078 470 92	-0.248 339 719	-0.890 127 107	H2	0.0	-1.879 800 64	2.057 660 28
C1	0.0	-0.854 485 593	2.311 978 65	H3	0.0	1.246 361 70	3.130 776 26
(c) Cl <sub>2</sub> ScH·C <sub>2</sub> H <sub>2</sub> Insertion Transition State							
CI Total Energy = -1 042.642 633							
Sc	0.0	0.351 269 058	0.104 067 410	C2	0.0	0.236 414 816	2.757 975 82
Cl1	-2.042 694 78	-0.135 523 913	-0.992 035 022	H1	0.0	1.631 674 90	1.379 397 00
Cl2	2.042 694 78	-0.135 523 913	-0.992 035 022	H2	0.0	-1.876 956 94	2.126 692 46
C1	0.0	-0.817 255 711	2.124 475 60	H3	0.0	1.033 374 38	3.457 332 97
(d) Cl <sub>2</sub> ScC <sub>2</sub> H <sub>3</sub> Vinyl Product							
CI Total Energy = -1 042.693 424							
Sc	0.0	-0.010 307 691 6	0.043 571 2767	C2	0.0	0.416 172 427	3.046 958 92
Cl1	-2.099 523 98	0.028 665 900 6	-1.037 483 62	H1	0.0	1.466 351 35	2.794 414 21
Cl2	2.099 523 98	0.028 665 900 6	-1.037 483 62	H2	0.0	-1.577 326 17	2.484 373 75
C1	0.0	-0.556 424 516	2.127 004 65	H3	0.0	0.225 459 606	4.106 181 17
(e) Cl <sub>2</sub> ScC <sub>2</sub> H <sub>3</sub> Acetylide Transition State							
CI Total Energy = -1 042.614 085							
Sc	0.0	0.311 680 895	-0.001 151 97782	C2	0.0	0.211 847 459	2.256 313 63
Cl1	-2.0594 348 7	-0.185 987 355	-1.025 125 12	H1	0.0	2.030 673 12	0.778 781 483
Cl2	2.0594 348 7	-0.185 987 355	-1.025 125 12	H2	0.0	-1.104 402 29	4.101 813 01
C1	0.0	-0.477 081 525	3.251 407 70	H3	0.0	1.416 515 80	1.652 575 64
(f) Cl <sub>2</sub> ScC <sub>2</sub> H·H <sub>2</sub> Acetylide Product							
CI Total Energy = -1 042.657 153							
Sc	0.0	-0.005 501 379 33	0.082 731 786 6	C2	0.0	-0.053 697 380 2	2.223 904 24
Cl1	-2.043 098 94	-0.049 322 881 0	-0.078 001 87	H1	0.0	2.586 211 00	-0.282 134 245
Cl2	2.043 098 94	-0.049 322 881 0	-0.078 001 87	H2	0.0	-0.058 657 219 5	4.492 858 07
C1	0.0	-0.060 061 217 6	3.438 709 36	H3	0.0	2.543 013 68	0.455 094 936
(g) Cl <sub>2</sub> ScC <sub>2</sub> H <sub>3</sub> H/D Exchange Transition State							
CI Total Energy = -1 042.598 326							
Sc	0.0	0.0	-0.018 348 8391	C2	0.0	0.0	2.365 148 62
Cl1	-2.084 413 98	0.0	-1.111 052 84	H1	0.0	-0.934 708 077	1.625 277 37
Cl2	2.084 413 98	0.0	-1.111 052 84	H2	0.0	0.0	4.651 470 09
C1	0.0	0.0	3.599 325 66	H3	0.0	0.934 708 077	1.625 277 37
(h) Cl <sub>2</sub> ScCH <sub>3</sub>							
CI Total Energy = -1 004.710 546							
Sc	0.0	-0.000 666 974	0.286 985 845	H1	0.0	1.016 622 60	2.847 365 60
Cl1	-1.913 292 23	0.000 336 788	-0.718 509 88	H2	0.0	-0.502 239 824	2.841 484 88
Cl2	1.913 292 23	0.000 336 788	-0.718 509 88	H3	0.0	-0.502 239 824	2.841 484 88
C	0.0	-0.000 510 818	2.451 601 02				
(i) Cl <sub>2</sub> ScC <sub>2</sub> H							
CI Total Energy = -1 041.521 529							
Sc	0.0	0.0	0.078 940 4342	C1	0.0	0.0	2.211 308 72
Cl1	-2.046 346 42	0.0	-1.068 579 4	C2	0.0	0.0	3.425 516 53
Cl2	2.046 346 42	0.0	-1.068 579 4	H1	0.0	0.0	4.479 390 51
(j) C <sub>2</sub> H <sub>2</sub> CI Total Energy = -76.962 652							
(k) H <sub>2</sub> CI Total Energy = -1.151 286							
(l) Mass-Weighted Cartesian Displacement Coordinates							

<sup>a</sup> Coordinates are in angstroms; energies are hartrees.

trically delocalized over centers A, B, and C. The one-electron orbital originally on center C moves to center A with an additional node being added during the course of the reaction to retain orthogonality to the orbital moving from center A to center C. The one-electron orbital on center M remains on center M during the course of the reaction but rehybridizes to retain overlap with the orbital moving from center C to center A. This rehybridization requires that there be an energetically accessible empty orbital of the correct shape on center M to rehybridize with the one-electron orbital on center M.

The alternative orbital pair motion involving motion of the orbitals on A and C is less common due to the lack of

virtual orbitals of low enough energy to participate in the essential rehybridization demanded by the Pauli principle, on either center A or center C. However, reactions 2 and 4, as reported here, have this type of orbital motion.

**II. Comparison of Electronic and Geometric Reorganizations.** To probe the generality of the overall orbital reorganization scheme outlined above and to understand the electronic differences for reactions 2–4, we have studied the electronic reorganizations that occur during the reaction of Cl<sub>2</sub>ScH with C<sub>2</sub>H<sub>2</sub> to form the vinyl product as in (2), the classical  $\beta$ -insertion reaction, the acetylide product as in reaction 4, and the saddle point for the degenerate  $\sigma$ -bond metathesis process as in reaction

Table II. Major Bond Distances and Bond Angles<sup>a</sup>

(a) $Cl_2ScH$			
Sc-Cl	2.348	H-Sc-Cl	114.27
Sc-H	1.755		
(b) $Cl_2ScH-C_2H_2$ Reactant			
Sc-Cl	2.360	Cl-Sc-Cl	123.49
Sc-H	1.768	H1-Sc-Cl	114.37
Sc-C1	2.751	C1-Sc-C2	24.77
Sc-C2	2.830	H1-Sc-C2	77.49
C1-C2	1.200	H2-C1-C2	172.75
C1-H2	1.056	H1-C2-C1	109.09
C2-H3	1.055	H3-C2-C1	179.75
(c) $Cl_2ScH-C_2H_2$ Insertion Transition State			
Sc-Cl	2.369	Cl-Sc-Cl	119.16
Sc-H	1.807	H1-Sc-C1	118.17
Sc-C1	2.334	C1-Sc-C2	27.57
Sc-C2	2.656	H1-Sc-C2	47.59
C1-C2	1.229	H2-C1-C2	148.86
C1-H2	1.060	H1-C2-C1	104.33
C2H1	1.961	H3-C2-C1	169.75
C2-H3	1.060		
H1-H3	2.162		
(d) $Cl_2ScC_2H_3$ Vinyl Product			
Sc-Cl	2.362	Cl-Sc-C1	125.48
Sc-H1	3.122	Cl-Sc-Cl	116.55
Sc-C1	2.154	Sc-Cl-C2	118.72
Sc-C2	3.034	C1-Sc-C2	22.77
C1-C2	1.339	H1-Sc-C2	20.15
C1-H2	1.082	H2-C1-C2	123.98
C2-H1	1.080	H1-C2-C1	123.07
C2-H3	1.076	H3-C2-C1	123.20
(e) $Cl_2ScC_2H_3$ Acetylide Transition State			
Sc-Cl	2.353	Cl-Sc-C1	122.13
Sc-C1	3.347	Cl-Sc-Cl	111.90
Sc-C2	2.260	C2-Sc-C1	115.17
Sc-H1	1.888	Sc-C2-C1	147.84
Sc-H3	1.989	H1-Sc-C2	68.13
C1-C2	1.210	H3-Sc-C2	36.28
C1-H2	1.057	H2-C1-C2	178.28
C2-H3	1.347	H3-C2-C1	151.31
H1-H3	1.068	H1-H3-C2	151.72
(f) $Cl_2ScC_2H_3$ Acetylide Product			
Sc-Cl	2.350	Cl-Sc-C1	120.76
Sc-C1	3.356	Cl-Sc-Cl	119.57
Sc-C2	2.142	C2-Sc-C1	119.56
Sc-H1	2.617	Sc-C2-C1	179.01
Sc-H3	2.576	H1-Sc-C2	99.30
C1-C2	1.215	H3-Sc-C2	82.98
C1-H2	1.054	H1-Sc-H3	16.33
C2-H3	3.142	H2-C1-C2	179.62
H1-H3	0.738	H3-C2-C1	124.56
		H1-H3-C2	127.62
(g) $Cl_2ScC_2H_3$ H/D Exchange Transition State			
Sc-Cl	2.353	Cl-Sc-C1	124.67
Sc-C2	2.383	C2-Sc-C1	117.66
Sc-H1	1.891	H1-Sc-H3	59.25
Sc-Cl	3.618	H1-Sc-C2	29.63
C1-C2	1.234	H1-C2-C1	128.36
C1-H2	1.052	H2-C1-C2	123.98
C2-H1	1.192	H2-C1-C2	180.00
		H1-C2-H3	103.27
(h) $Cl_2ScCH_3$			
Sc-Cl	2.365	C-Sc-Cl	115.16
Sc-C	2.165	Sc-C-H <sub>p</sub>	111.27
C-H	1.090	Sc-C-H	110.97

<sup>a</sup>Distances are in angstroms; angles are in degrees.

3. In subsection A below, we discuss the geometries of the equilibrium structures. In subsection B we discuss the geometry changes and sketch the geometric and electronic reorganization that occurs in the classical  $\beta$ -insertion reaction 2. In subsection C we discuss the geometry changes and sketch the electronic reorganization that occurs in the

acetylide formation reaction 4. In subsection D we outline the unique geometric and electronic features of the H/D exchange process 3 for acetylenes.

**A. Equilibrium Structures.** The unconstrained geometry obtained in the present study with analytic gradients and a Hartree-Fock wave function for  $Cl_2ScH$  is similar to the constrained geometry found previously by Steigerwald and Goddard for the same complex.<sup>4a</sup> We find (see Table II) a Sc-H distance of 1.76 Å, a Sc-Cl distance of 2.35 Å, and a Cl-Sc-Cl angle of 133.5° (Stiegerwald and Goddard report 1.78, 2.35 Å, with a fixed angle of 142°). For  $Cl_2ScCH_3$  we find a perfectly conventional structure. The calculated Sc-C distance is 2.17 Å; the experimental Sc-C distance for  $Cp^*_2ScCH_3$  is 2.243 (11) Å.<sup>1c</sup> The three Sc-C-H angles are all nearly 111°. The Sc-C-H angle for the H in the equatorial plane of the wedge is slightly different from the other two (0.3° larger) as there were no equivalence constraints applied. There is no evidence for an agostic interaction for this system, in accord with the recent theoretical study by Williamson and Hall on  $Cl_3-TiCH_3$ .<sup>4i</sup> We find the anticipated shrinkage in the Sc-C bond distance upon changing from an  $sp^3$  carbon (2.17 Å for methyl) to an  $sp^2$  carbon (2.15 Å for vinyl) to an  $sp$  carbon (2.13 Å for acetylide). The C-C bond distances found for the vinyl and acetylide complexes of 1.34 and 1.21 Å are as would be expected for typical C-C double and triple bonds, respectively. The Sc-C-C angles of 119° and 180° are also typical for bond angles at  $sp^2$  and  $sp$  centers, respectively.

**B. Classical  $\beta$ -Insertion Reaction.** It is generally accepted<sup>5,6</sup> that the insertion of metal-ligand  $\sigma$  bonds into C-C  $\pi$  bonds occurs through a prior coordination of the  $\pi$  bond onto the metal center followed by a  $2\pi + 2\sigma$  reaction involving the C-C  $\pi$  bond and the metal-ligand  $\sigma$  bond. Previous theoretical studies<sup>4c,g,5</sup> have focused on the more common insertion reaction involving olefinic  $\pi$  bonds. The general analysis given by Thorn and Hoffmann<sup>5</sup> should be directly applicable to acetylenic  $\pi$  bonds.

For our  $Cl_2ScH$  system, we find the saddlepoint for acetylene insertion to be rather early, the C-C bond has only lengthened 0.03 Å, the Sc-H bond has lengthened 0.04 Å, and the newly forming C-H bond has a distance of 1.961 Å (compared to a final C-H distance of 1.080 Å).

The valence orbitals for the reactant acetylene complex (Figure 1a-d) are as would be expected for a weak Lewis acid-base complex since the metal center lacks an appropriate pair of electrons for Dewar-Chart-Duncanson back bonding.<sup>6</sup> The  $\pi$ -bond pair involved in the Lewis acid-base interaction is plotted in Figure 1a,b—the delocalization onto the metal center is small. The Sc-H  $\sigma$ -bond pair is plotted in Figure 1c,d. The hydrogen one electron orbital is in Figure 1c, and the Sc  $d_z$  orbital is plotted in Figure 1d.

As discussed in section I, two of the four orbitals do remain on their initial atomic centers during the reaction and two do flow across in response to bonding changes that occur during the reaction. One of the carbon p orbitals (initially in the C-C  $\pi$  bond) remains on its center and rehybridizes into a  $sp^n$  hybrid orbital that is spin paired to the Sc in the product vinyl complex (compare Figure 1a with Figure 1e and Figure 1i). The second orbital that remains fixed is the hydrogen s orbital; it is initially bonded to Sc and finally bonded to a  $sp^n$  hybrid orbital (compare Figure 1c with Figure 1g and Figure 1k). The remaining two orbitals switch centers as the C-C  $\pi$  bond changes into a Sc-C  $\sigma$  bond, and the Sc-H  $\sigma$  bond changes into a C-H  $\sigma$  bond. The transition state occurs early enough so that only a small amount of delocalization has occurred by the saddle point, but a comparison of Figure 1b with Figure

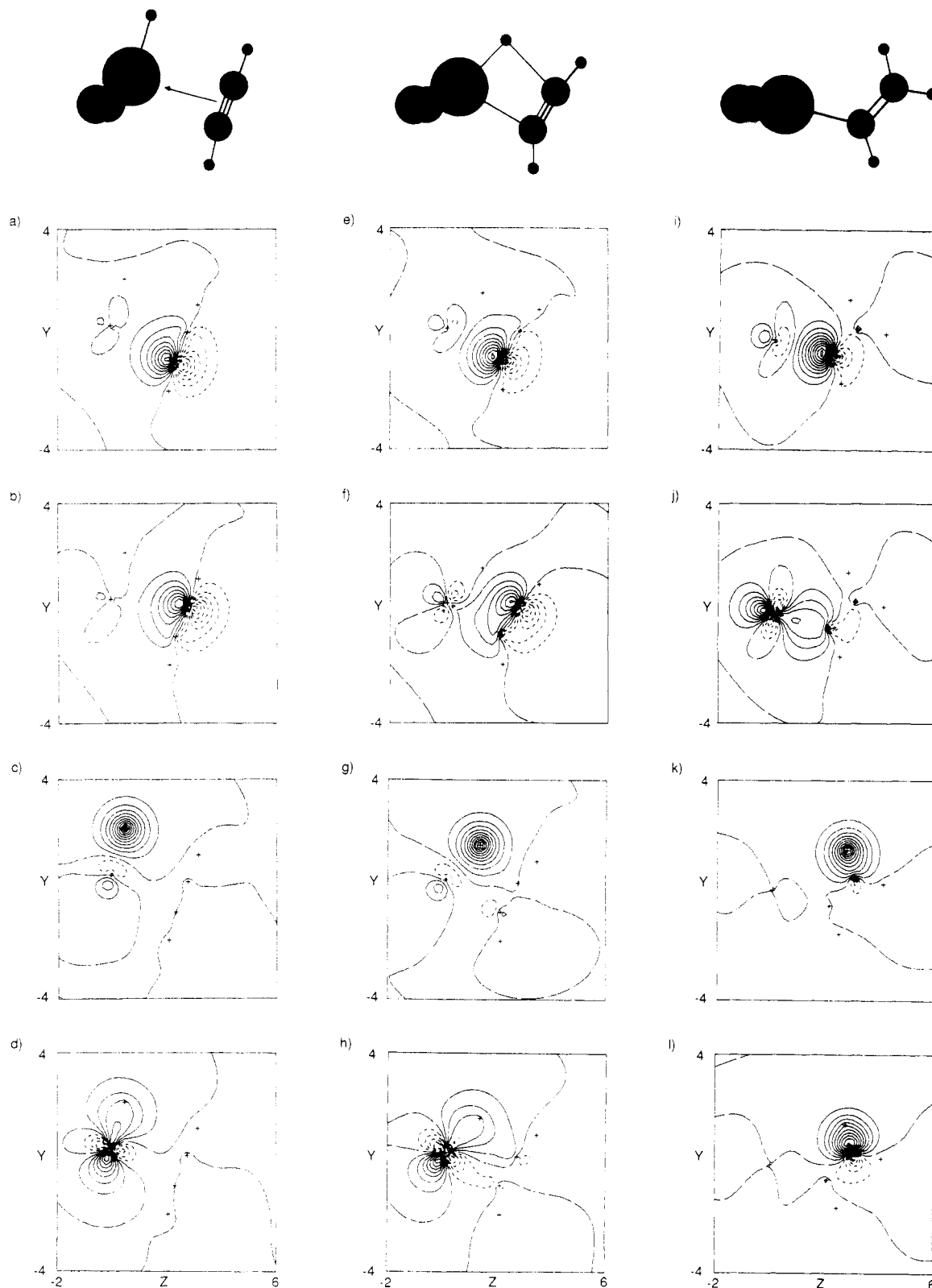


**Figure 1.** Contour plots of the GVB orbitals defining the one-electron orbitals of the complexed acetylene (a-d), the saddle point (e-h), and the vinyl product (i-l) for the classical  $\beta$ -insertion pathway. The plotting plane for each orbital contains all of the active centers (Sc, the two carbons, and all three hydrogens). The solid contours define positive orbital amplitude (spaced / .05 au), the dashed contours define negative orbital amplitude, and the long dashed lines define nodal lines. (a,e,i) The C  $\pi$  one-electron orbital (of the first singlet coupled pair), which remains on its original center. (b,f,j) The C  $\pi$  one-electron orbital, which symmetrically delocalizes onto a scandium center (of the first singlet coupled pair). (c,g,k) The H  $\sigma$  one-electron orbital (of the second singlet-coupled pair), which remains on its original center. (d,h,l) The Sc  $\sigma$  one-electron orbital (of the second singlet-coupled pair), which delocalizes onto the terminal carbon of the vinyl product.

1f and Figure 1j demonstrates the ease with which the C-C  $\pi$  bond is changed into a Sc-C  $\sigma$  bond. Comparison of Figure 1e with 1f shows the retention of overlap for this bond pair during the course of reaction. The transfer-

mation of the Sc-H  $\sigma$  bond into a C-H  $\sigma$  bond is shown in Figure 1d,h,j. From a comparison of Figure 1g with 1h one can see the retention of overlap for this bond pair during the course of reaction.

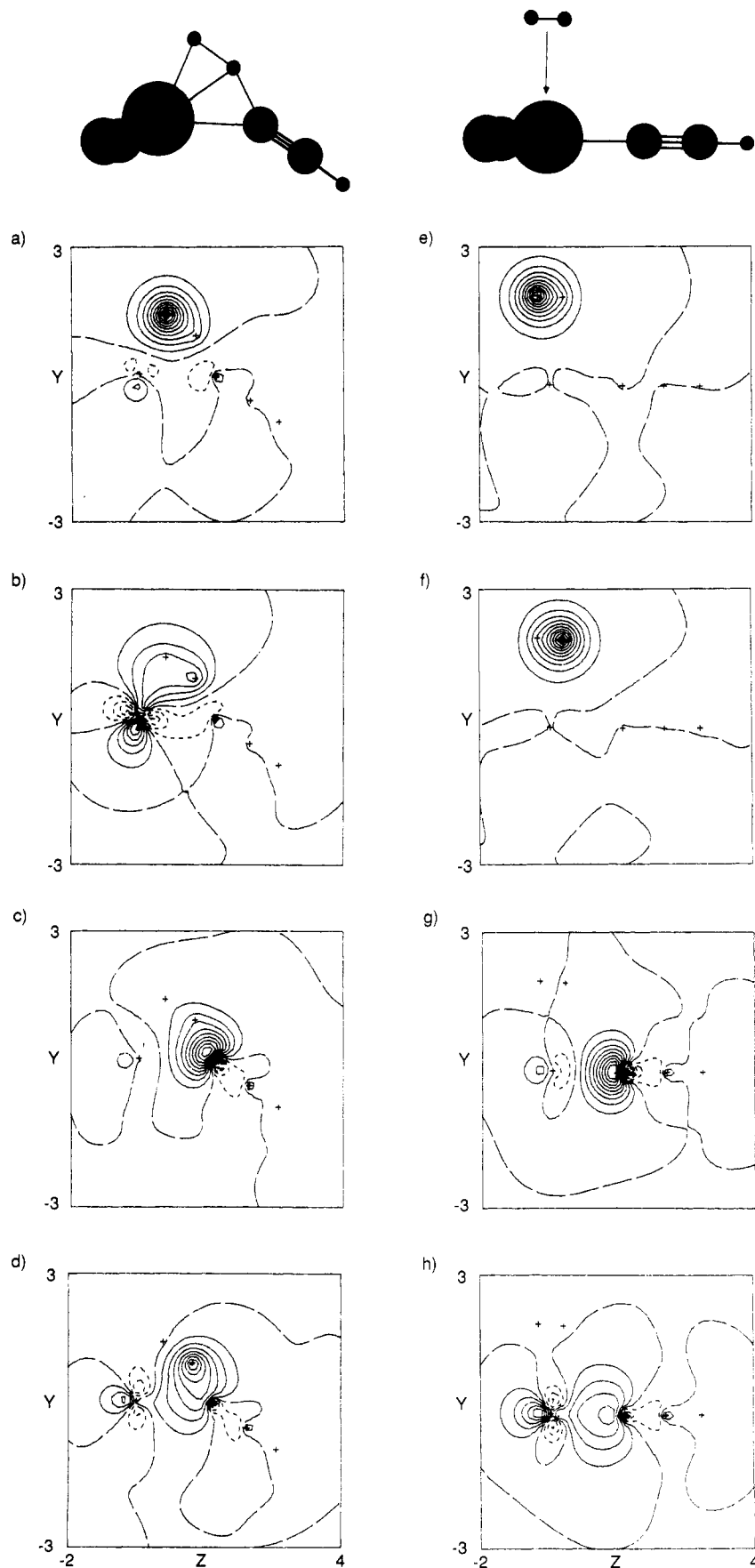


**Figure 2.** Contour plots of the GVB orbitals defining the one-electron orbitals of the saddlepoint (a-d) and the acetylide product (e-h) of the acetylide-forming  $\sigma$ -bond metathesis pathway. The plotting plane for each orbital contains all of the active centers (Sc, the two carbons, and all three hydrogens). The solid contours define positive orbital amplitude (spaced 0.05 au), the dashed contours define negative orbital amplitude, and the long dashed lines define nodal lines. (a,e) The H  $\sigma$  one-electron orbital originally bonded to Sc and finally bonded to H (of the first singlet-coupled pair), which remains on its original center. (b,f) The Sc  $\sigma$  one-electron orbital, which delocalizes onto the H, which forms a  $H_2$  center (of the first singlet-coupled pair). (c,g) The C  $\sigma$  one-electron orbital (of the second singlet-coupled pair), which remains on its original center, originally bonded to H and ultimately bonded to Sc. (d,h,i) The H  $\sigma$  one-electron orbital (of the second singlet-coupled pair), which delocalizes onto Sc in the acetylide product.

**Table III. Exchange Reaction Coordinates (Mass-Weighted Cartesian Displacement Coordinates (angstroms)) at Frequency =  $-718.8\text{ cm}^{-1}$** 

atom	X	Y	Z
Sc	0.0	-0.009363	-0.000006
Cl1	0.000247	0.005249	-0.000052
Cl2	-0.000247	0.005249	-0.000052
C1	0.0	-0.011366	-0.003590
C2	0.0	0.046934	0.004670
H1	0.0	-0.163579	0.196123
H2	0.0	0.925749	0.001757
H3	0.0	-0.175423	-0.210903

**C. Acetylide Formation through  $\sigma$ -Bond Metathesis.** It has previously been suggested that the formation of either  $\text{H}_2$  or  $\text{CH}_4$  from reaction of terminal acetylenes with  $\text{Cp}^*\text{ScH}$  or  $\text{Cp}^*\text{ScCH}_3$ , respectively, occurs through a covalent four-center  $2\sigma + 2\sigma$  reaction.

We find the saddlepoint to be the result of a direct interaction of the C-H bond of acetylene with the Sc-H bond of  $\text{Cl}_2\text{ScH}$  as evidenced from the geometry shown in the first column of Figure 2. It is interesting to note that this direct approach of hydrocarbon has been suggested for reactions of hydrocarbons with coordinately unsaturated group VIII transition metal complexes<sup>3</sup> (the only other class of transition metal complexes observed to directly react with external sources of C-H bonds). Further, it is apparent that the saddlepoint is intermediate between reactants and products and is quite similar to that reported previously for  $\sigma$ -bond metathesis processes.<sup>4a</sup> The Sc-H bond has lengthened from 1.77 to 1.89 Å. For the  $\text{Cl}_2\text{ScH}_3$  saddlepoint, the Sc-H bond lengthens to 1.88 Å. The C-H bond has lengthened from 1.06 to 1.35 Å. The H-H distance is 1.07 Å compared to 0.74 Å in the product. The C-H-H angle is 151.72° for the  $\text{Cl}_2\text{ScH}(\text{C}_2\text{H}_2)$  saddlepoint; for the  $\text{Cl}_2\text{ScH}_3$  saddlepoint the H-H-H angle is 146.7°.

As discussed in section I, two of the four orbitals remain on their initial atomic centers during the reaction and two flow across in response to bonding changes that occur during the reaction. One of the orbitals that remains fixed is the hydrogen s orbital it is initially bonded to Sc and finally bonded to the other hydrogen orbital (see Figure 2a and 2e). The second orbital that remains fixed is the carbon "sp" hybrid orbital (initially in the C-H  $\sigma$  bond); it remains on its center and retains its "sp" hybridization when it is spin paired to the Sc in the product acetylide complex (see Figure 2c and 2g). The remaining two orbitals switch centers as the C-H  $\sigma$  bond changes into a Sc-C  $\sigma$  bond and the Sc-H  $\sigma$  bond changes into a H-H  $\sigma$  bond. The transition state occurs far enough along the reactions coordinate that a substantial amount of delocalization has occurred by the saddle point (see Figure 2b and 2d). Comparison of Figure 2a with 2b and Figure 2c with 2d shows the retention of overlap for both bond pairs during the course of reaction.

**D. H/D Exchange for Acetylenes.** The H/D exchange reaction for hydrogen at a scandium center has been thoroughly studied experimentally<sup>1,2</sup> and theoretically.<sup>4a,h,7</sup> Rapid H/D exchange has been observed for  $\text{H}_2$ , arenes, primary C-H bonds, and cyclopropane; slower exchange is observed for secondary C-H bonds. Alkenes undergo rapid H/D exchange. However, for alkynes the H/D is not observed, and only the  $\beta$ -insertion and acetylide reaction paths have been observed.<sup>1</sup>

The saddlepoint (as determined by normal-mode analysis; see Table III) calculated for this process is certainly geometrically related to those for other  $\sigma$ -bond

metathesis reactions, but it has some rather distinct features that will be discussed below. The Sc-H bonds lengthen from 1.77 to 1.89 Å for  $\text{Cl}_2\text{ScH}(\text{C}_2\text{H}_2)$  and to 1.88 Å for the  $\text{Cl}_2\text{ScH}_3$  saddlepoint. The H-C-H angle is 103.27° for  $\text{Cl}_2\text{ScH}(\text{C}_2\text{H}_2)$ , substantially different than for the  $\text{Cl}_2\text{ScH}_3$  saddlepoint, where the H-H-H angle is 146.7°.

The electronic reorganization discussed in subsection A for the general case is precisely what has been calculated for the  $\text{Cl}_2\text{ScH}$  plus  $\text{H}_2$  case. In fact, the Steigerwald and Goddard study<sup>4a</sup> of this system was the first illustration of the general phenomena discussed in subsection A. For the reaction involving  $\text{Cl}_2\text{ScH}(\text{C}_2\text{H}_2)$  an additional pair of electrons must be considered—the in-plane C-C  $\pi$  bond. A comparison of bond strengths between C-C  $\pi$  bonds, C-H  $\sigma$  bonds, and Sc-H  $\sigma$  bonds is adequate to explain the preferred bonding scheme shown in Figure 3. The lowest energy pair (fewest nodes) is a symmetric C-H bond pair. The second lowest energy pair (a single additional node) is an antisymmetric C-H bond pair. The remaining pair of electrons is in a  $\pi$  bond between the scandium and the  $\beta$ -carbon atom. The energetic consequences of the repulsive interactions resulting from the addition of the third pair of electrons are discussed in section III. The reaction has a higher activation barrier than those calculated for the  $\beta$ -insertion and acetylide-forming  $\sigma$ -bond metathesis reactions and hence should not be experimentally observed.<sup>1</sup>

**III. Reaction Energetics.** As discussed above, the only reaction path that is calculated to include prior acetylene coordination is the classical  $\beta$ -insertion reaction. The reaction profile for this process is shown in Figure 4a. Given a calculated  $\Delta H$  of -15.4 and a  $\Delta G_{300}$  of -4.0 kcal/mol, it would be expected that there would be a modest buildup of alkyne complex in solution (depending upon the solubility of alkyne in the chosen solvent and the additional sterics associated with permethylcyclopentadienyl ligands). The activation energy for vinyl formation is only 6.3 kcal/mol with respect to complexed alkyne. Referenced to free acetylene, the activation energy is -9.1 kcal/mol. The small barrier is in general agreement with experimental results and previous theoretical studies on olefin insertion.<sup>1,4-6</sup> The exothermicity of 36.5 kcal/mol with respect to free acetylene would suggest that this reaction would be only slightly reversible for the sterically unencumbered chloride ligand set.

The reaction profile for the acetylide forming  $2\sigma + 2\sigma$  reaction is shown in Figure 4b. Again, the reaction barrier is quite small, only 6.2 kcal/mol with respect to free acetylene. The smaller exothermicity of this reaction ( $\Delta H = -15.2$  kcal/mol) relative to the  $\beta$ -insertion reaction above would suggest that this reaction is more reversible than the insertion reaction.

The reaction profile for the simple H/D exchange process is shown in Figure 4c. For this case we calculate a barrier of 13.7 kcal/mol, twice as large as for either of the other two pathways. As discussed in section II.C, the orthogonality constraints imposed by the presence of the C-C  $\pi$  bond are the likely cause for the height of this barrier relative to the other two pathways in Figure 4a and 4b.

In light of the small barriers but differing exothermicities calculated for the alkyne  $\beta$ -insertion and acetylide-formation reactions and the observed difference in reactivities of Sc-H and Sc-R bonds,<sup>1</sup> we calculated the overall exothermicities for the two pathways for  $\text{Cl}_2\text{ScCH}_3$  as the reactant. The  $\beta$ -insertion reaction is calculated to be 39.1 kcal/mol exothermic and the acetylide-forming reaction is calculated to be 40.9 kcal/mol exothermic. The calculated  $\Delta\Delta H$  of only 1.8 kcal/mol for the  $\text{Cl}_2\text{Sc}-\text{CH}_3$  case is

(7) Brintzinger, H. H. *J. Organomet. Chem.* 1979, 171, 337.

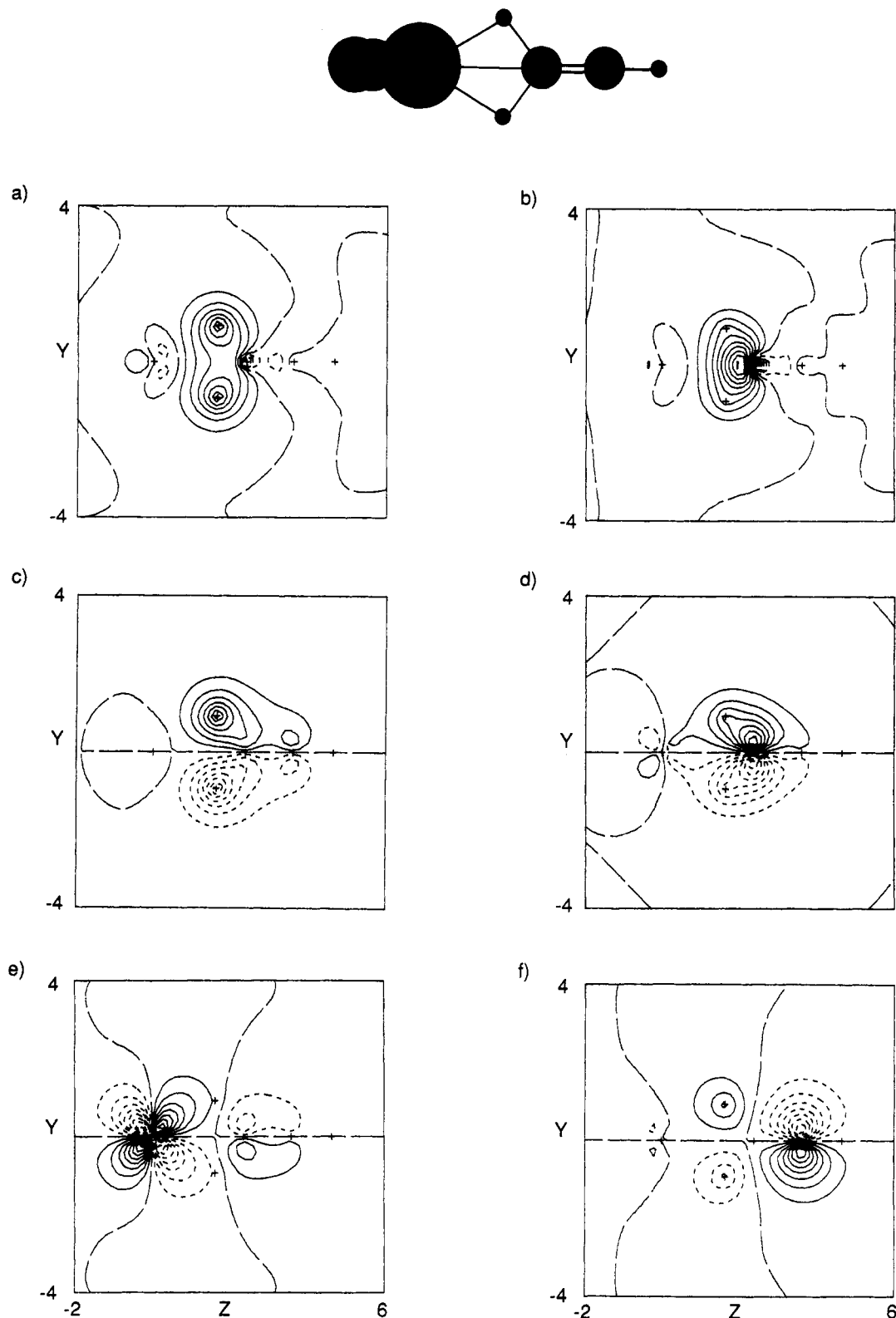


**Figure 3.** Contour plots of the six GVB orbitals defining the active one-electron orbitals of the H/D exchange  $\sigma$ -bond metathesis pathway. The plotting plane for each orbital contains all of the active centers (Sc, the two carbons, and all three hydrogens). The solid contours define positive orbital amplitude (spaced 0.0k au), the dashed contours define negative orbital amplitude, and the long dashed lines define nodal lines. (a,b) The totally symmetric C-H bond pair. (c,d) The antisymmetric C-H bond pair. (e,f) The residual pair of electrons forming a singlet-coupled pair between Sc and the terminal carbon.

in sharp contrast to the calculated  $\Delta\Delta H$  of 21.3 kcal/mol for the  $\text{Cl}_2\text{Sc-H}$  cases discussed above. Given the similarities in Sc-H and Sc-C bond strengths discussed in the literature<sup>8</sup> and the similarity in the H-H and C-H bond

strengths of the  $\text{H}_2$  and  $\text{CH}_4$  ( $D_0(\text{H}_2) = 103.29$  kcal/mol,<sup>9a</sup>  $D_0(\text{CH}_3\text{H}) = 103.25$  kcal/mol<sup>9b</sup>), the products of the ace-

(8) Labinger, J. A.; Bercaw, J. E. *Organometallics* 1988, 7, 926-928.

(9) (a) Huber, K. P.; Herzberg, G. *Molecular Spectra and Molecular Structure IV. Constants of Diatomic Molecules*; Van Nostrand Reinhold: New York, 1979. (b) Stull, D. R.; Prophet, H. *Natl. Stand. Ref. Data Ser., Natl. Bur. Stand. (U.S.)* 1971, 37.



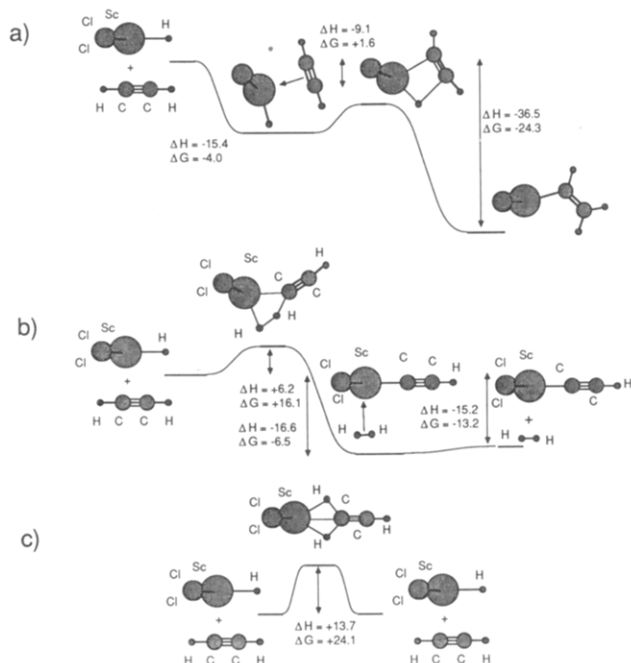


**Figure 4.** Reaction energy diagrams for the reactions of acetylene with  $\text{Cl}_2\text{ScH}$ . (a) The classical  $\beta$  insertion pathway. (b) The acetylide-forming  $\sigma$ -bond metathesis pathway. (c) The H/D exchange  $\sigma$ -bond metathesis pathway. The energies are obtained from the CI calculations and are in kcal/mol.

tylide-forming reaction this difference of  $\Delta\Delta H$ 's can be attributed to the significant difference between the C-H bond in the vinyl product and the C-C single bond in the propenyl product. For example, for the parent ethylene/propylene comparison the  $\Delta D_0$  for the C-H and C-C bonds is 8 kcal/mol.<sup>9b</sup>

**IV. Discussion and Conclusions.** For the three reactions of acetylene with  $\text{Cl}_2\text{ScH}$  that were studied, we find that the classical insertion pathway is significantly favored over the two  $\sigma$ -bond metathesis pathways, one resulting in H/D exchange and the other resulting in formation of a scandium acetylide. Given the reversibility of the acetylide-forming reaction, H/D exchange could occur through sequential formation and reduction of the acetylide complex. The insertion pathway was the only one calculated to proceed through a metal-acetylene complex. The two  $\sigma$ -bond metathesis pathways were each calculated to proceed through a direct interaction with the Sc-H bond. The direct H/D exchange reaction was found to have the highest barrier. In addition, the overall reaction energetics were calculated for the insertion and acetylide formation reactions of  $\text{Cl}_2\text{ScCH}_3$  with acetylene. In contrast to the hydride reactions, the insertion and acetylide formation reactions for the methyl complex were found to be equivalently exothermic.

The anticipated (and obtained) preference for the  $\beta$ -insertion pathway over either of the two  $\sigma$ -bond metathesis pathways is in contradiction to experimental reality. Bercaw and co-workers<sup>1</sup> have observed that  $\text{Cp}^*_2\text{Sc-R}'$  ( $\text{R}' = \text{H}, \text{CH}_3$ ) reacts with propyne to form exclusively the  $\sigma$ -bond metathesis product acetylide instead of the classical  $\beta$ -insertion product. We obtain the expected result that prior coordination of the  $\pi$  bond does lower the overall barrier. The two  $\sigma$ -bond metathesis reactions were calculated to proceed through direct pathways and are hence not stabilized by the  $\pi$  complexation energy. This apparent disagreement between experiment and theory is as found previously.<sup>3b</sup> As discussed in the Introduction, Stoutland and Bergman<sup>3</sup> have shown that ethylene reacts

with the coordinatively unsaturated intermediate  $\text{Cp}^*\text{Ir}(\text{PMe}_3)$  to preferentially form a vinyl hydride rather than the expected olefin adduct through an independent pathway. This preferential formation of a product that occurs through a reaction path that must have an intrinsic activation barrier (breakage and formation of covalent bonds), instead of a product that occurs through a reaction path that is recognized to involve very little electronic reorganization, runs counter to both intuition and theoretical studies.<sup>3b</sup> Extended Hückel calculations suggest that the vinyl hydride forming reaction has a barrier at least 10 kcal/mol larger than that for forming the olefin adduct.

One possible explanation for this apparent disagreement between experiment and theory is that the reaction involves intimate solvent participation<sup>10</sup> wherein the attacking alkene or alkyne must displace a coordinated solvent molecule if prior coordination is required but not if direct reaction is possible.

An alternate explanation (posed by Hoffmann, Bergman, and co-workers<sup>3b</sup>) is that there is a dynamical difference between the pathways. The coordination event requires a rather specific orientation to proceed, whereas the direct reaction is conformationally more flexible.

A third explanation (posed by a referee) is that the steric differences between Cl and  $\text{Cp}^*$  differentially affect the prior coordination of the acetylene. If the energy of prior coordination is subtracted from the energetic profile in Figure 4a, then  $\beta$  insertion and acetylide formation become competitive energetically. Preliminary molecular mechanics calculations tend to support this alternative. If the atoms in the equatorial plane are held fixed at the ab initio coordinates but the atoms in the Cl, Cp, or  $\text{Cp}^*$  groups are minimized by using an empirical force field, the effect on the binding energy of acetylene is 1.1 kcal/mol for Cp but 11.1 kcal/mol for  $\text{Cp}^*$ .

**V. Computational Details. A. Basis Sets and Effective Potentials.** All of the calculations reported here were carried out using Cartesian-Gaussian basis sets. For Cl<sup>11</sup> an effective core potential was used to replace the core electrons, allowing self-consistent orbital optimization to be carried out only for the valence electrons. For Sc<sup>12</sup> an effective potential was used to replace the 1s, 2s, and 2p orbitals, again reducing the number of functions for the self-consistent orbital optimization. For geometry optimizations a (7s,4p/3s,3p) basis set was used for carbon.<sup>13</sup> A (6s/3s) basis, unscaled, was used for the hydrogens in  $\text{H}_2$  or bound to the metal.<sup>14</sup> A (4s/2s) basis, scaled, was used for the hydrogens not participating in the reaction.<sup>14</sup> For the final series of calculations used to determine the energetics, the Dunning/Huzinaga<sup>15</sup> valence double- $\zeta$  carbon basis set was used, augmented with a set of d Gaussians ( $\zeta = 0.75$ ).<sup>15</sup> The unscaled triple- $\zeta$  hydrogen basis was augmented with a single set of p Gaussians ( $\zeta = 0.6$ ) for the final series of calculations. For chlorine, a valence minimum basis (3s,3p/1s,1p)<sup>11</sup> was used for all calculations. For Sc, a valence double- $\zeta$  (6s,5p,5d/3s,3p,2d) basis<sup>12,16</sup> was used for all calculations.

(10) Martin, B. D.; Warner, K. E.; Norton, J. R. *J. Am. Chem. Soc.* **1986**, *108*, 33-39.

(11) Rappé, A. K.; Smedley, T. A.; Goddard, W. A. *J. Phys. Chem.* **1981**, *85*, 1662-1666.

(12) Hay, P. J.; Wadt, W. R. *J. Chem. Phys.* **1985**, *82*, 270-283.

(13) Rappé, A. K.; Goddard, W. A., manuscript in preparation.

(14) Huzinaga, S. *J. Chem. Phys.* **1965**, *42*, 1293.

(15) Dunning, T. H.; Hay, P. J. In *Modern Theoretical Chemistry: Methods of Electronic Structure Theory*; Schaefer III, H. F., Ed.; Plenum Press: New York, 1977; Vol. 3, Chapter 1, pp 1-27.

(16) Rappé, A. K.; Smedley, T. A.; Goddard, W. A. *J. Phys. Chem.* **1981**, *85*, 2607-2611.

**B. Wave Functions.** The geometries of the stationary points were generated with analytic gradient techniques using restricted Hartree-Fock wave functions. For the final optimized geometries, GVB wave functions<sup>17</sup> were obtained, and CI calculations<sup>18</sup> were performed consisting of RCI quadruples plus a Pol(2/1)-CI<sup>19</sup> including the GVB orbitals and the entire virtual space. For each structure all of the valence electrons on carbon, hydrogen, and scandium were correlated.

**C. Geometry Optimizations.** As mentioned above, the geometries of the reactants, transition states, and products were determined by using analytic derivatives of the form

$$d_{li} = \partial E(\Psi_{\text{HF}}) / \partial q_{li}$$

for all Cartesian coordinates  $q_l$  of each atom  $i$  in the molecule, using the numerical procedure of Dupuis and King.<sup>20</sup> Second derivatives  $k_{li,mj}$  were estimated by using Badger's rules<sup>21</sup> and updated with finite difference of the first derivatives at each geometry by using a procedure implemented by Upton and Rappé.<sup>22</sup> Assuming the total potential near the minimum to be of the form

$$V(\mathbf{r}) = V_0 + \mathbf{d} \cdot \mathbf{r} + \frac{1}{2} \mathbf{k} \cdot \mathbf{r}^2$$

(17) Bobrowicz, F. W.; Goddard, W. A. In *Modern Theoretical Chemistry: Methods of Electronic Structure Theory*; Schaefer III, H. F., Ed.; Plenum Press: New York, 1977; Vol. 3, Chapter 4, pp 79-127.

(18) Shavitt, I. In *Modern Theoretical Chemistry: Methods of Electronic Structure Theory*; Schaefer III, H. F., Ed.; Plenum Press: New York, 1977; Vol. 3, Chapter 6, pp 189-275.

(19) Hay, P. J.; Dunning, T. H. *J. Chem. Phys.* 1976, 64, 5077.

(20) Dupuis, M.; King, H. F. *J. Chem. Phys.* 1978, 68, 3998-4004.

(21) Badger, R. M. *J. Chem. Phys.* 1934, 2, 128-131; *Ibid.* 1935, 3, 710-714.

(22) Rappé, A. K.; Upton, T. H. *Organometallics*, 1984, 3, 1440-1442. Upton, T. H.; Rappé, A. K. *J. Am. Chem. Soc.* 1985, 107, 1206-1218.

the global minimum in the potential was found by using successive Newton-Raphson steps,<sup>23</sup>  $\Delta \mathbf{r} = -\mathbf{d}/\mathbf{k}$  to define new test geometries. To locate the transition state, the Lagrange multiplier technique of Simons and co-workers<sup>24</sup> was used. The final geometries and CI total energies are collected in Table I. For each equilibrium structure six zero eigenvalues were found corresponding to the translational and rotational degrees of freedom—the remaining eigenvalues were positive. For the saddlepoint structures a single negative eigenvalue was obtained corresponding to the reaction coordinate, six zero eigenvalues were found corresponding to the translational and rotational degrees of freedom, and the remaining eigenvalues were positive.

For the acetylide transition state where a  $C_{2v}$  saddlepoint was found, steps away from  $C_{2v}$  symmetry were carried out to assess whether or not the  $C_{2v}$  structure was indeed a saddlepoint or merely an arbitrary point on the potential energy surface or an equilibrium structure. The single negative eigenvalue found was indeed for a distortion from  $C_{2v}$  to  $C_s$  symmetry. In contrast to the work of Steigerwald and Goddard<sup>4a</sup> for the parent  $\text{Cl}_2\text{ScH} + \text{H}_2$  case, the reaction coordinate here (not surprisingly) predominately consists of motion of the terminal hydrogen of the acetylene. The eigenvector corresponding to the reaction coordinate is given in Table III.

**Acknowledgment.** This work is supported by NSF Grant CHE-8405399. Acknowledgment is made to the CSU Supercomputing Project for partial support of this research.

(23) Schlegel, H. B. *J. Comput. Chem.* 1982, 3, 214-218.

(24) Simons, J.; Jorgensen, P.; Taylor, H.; Ozment, J. *J. Phys. Chem.* 1983, 87, 2745-2753.

## Dimethyl Sulfide Substituted Mixed-Metal Clusters: Synthesis, Structure, and Characterization of $\text{HRuCo}_3(\text{CO})_{11}(\text{SMe}_2)$ and $[\text{HRuRh}_3(\text{CO})_9]_2[\text{SMe}_2]_3$

Sirpa Rossi, Jouni Pursiainen, Markku Ahlgren, and Tapani A. Pakkanen\*

Department of Chemistry, University of Joensuu, P.O. Box 111, Joensuu, SF-80101 Finland

Received March 14, 1989

Ligand substitution reactions of dimethyl sulfide with mixed-metal clusters are described. The clusters  $\text{HRuCo}_3(\text{CO})_{11}(\text{SMe}_2)$  (1) and  $[\text{HRuRh}_3(\text{CO})_9]_2[\text{SMe}_2]_3$  (2) have been prepared by reactions of  $\text{SMe}_2$  with the neutral parent clusters. Their crystal structures have been established: 1, monoclinic, space group  $P2_1/n$ ,  $a = 11.459$  (5) Å,  $b = 12.484$  (4) Å,  $c = 14.384$  (4) Å,  $\beta = 96.40$  (3)°,  $Z = 4$ ; 2, trigonal, space group  $R\bar{3}c$ ,  $a = 13.181$  (7) Å,  $\alpha = 75.54$  (5)°,  $Z = 2$ . Dimethyl sulfide coordinates terminally as a two-electron donor on basal cobalt in 1 and as a bridging four-electron donor causing unusual dimerization of clusters in 2. The carbonyl arrangement of the parent clusters was not changed during the ligand substitution, and hydride ligands bridge the three basal metals in both compounds.

### Introduction

Mixed-metal clusters and their ligand substitution reactions have been studied extensively. Among the most commonly used ligands are phosphines and phosphites, but also a variety of sulfur ligands have been employed.<sup>1</sup> Reactions of metal clusters with sulfur-containing ligands

are important, when catalytic processes are studied, sulfur being one of the foremost catalyst poisons.<sup>2</sup>

Sulfur ligands can be classified as  $\text{S}^{2-}$ ,  $\text{SR}^-$ , or  $\text{SR}_2$  analogues.  $\text{S}^{2-}$  or elemental sulfur is commonly found to

(1) Wilkinson, G.; Stone, F. G. A.; Abel, E. W. *Comprehensive Organometallic Chemistry*; Pergamon: Oxford, England, 1982.

(2) Rakowski DuBois, M. *Chem. Rev.* 1989, 89, 1.

\* To whom correspondence should be addressed.